

~~CONFIDENTIAL~~

CC 78
RM L54A29

NACA RM L54A29



c.1

~~CONFIDENTIAL~~
NACA

RESEARCH MEMORANDUM

TRANSONIC WIND-TUNNEL INVESTIGATION OF THE EFFECTS OF
BODY INDENTATION ON THE AERODYNAMIC CHARACTERISTICS
OF A SEMIELLIPTICAL SWEEPBACK WING-ROOT
INLET CONFIGURATION

By Arvid L. Keith, Jr.

Langley Aeronautical Laboratory
CLASSIFICATION CHANGED ~~CONFIDENTIAL~~ Langley Field; Va.

UNCLASSIFIED

To: _____
By authority of: *NACA Reel also effective*
+ RN-121 *Feb. 14, 1957*
DECLASSIFIED DOCUMENT

This material contains information affecting the National Defense of the United States within the meaning of the espionage laws, Title 18, U.S.C., Sec. 793 and 794, the transmission or revelation of which in any manner to an unauthorized person is prohibited by law.

NATIONAL ADVISORY COMMITTEE
FOR AERONAUTICS

WASHINGTON
March 25, 1954

APR 11 1954

~~CONFIDENTIAL~~

NATIONAL ADVISORY COMMITTEE FOR AERONAUTICS

RESEARCH MEMORANDUM

TRANSONIC WIND-TUNNEL INVESTIGATION OF THE EFFECTS OF
BODY INDENTATION ON THE AERODYNAMIC CHARACTERISTICS
OF A SEMIELLIPTICAL SWEEPBACK WING-ROOT
INLET CONFIGURATION

By Arvid L. Keith, Jr.

SUMMARY

An investigation has been conducted in the Langley transonic blowdown tunnel between Mach numbers of 0.65 and 1.4 to determine whether the principles of the transonic area rule could be used to improve the transonic drag-rise characteristics of a semielliptical shaped sweptback air inlet installed in the root of a 45° sweptback-wing-body combination. The results show that indenting the fuselage of the inlet configuration an amount equal to the total area added by the inlet installation less the area of an entering free-stream tube at the design mass-flow ratio of 0.80, eliminated the small increment in transonic drag caused by the inlet installation. The drag coefficient of the indented inlet configuration at most supersonic Mach numbers was less than that of either the basic or the original inlet configuration at both lifting and nonlifting conditions. Indications were that the indented configuration would have less drag to Mach numbers somewhat higher than the test limit.

INTRODUCTION

The transonic drag-rise characteristics of wing-body combinations have been shown in reference 1 to be primarily dependent upon the axial distribution of cross-sectional area. This concept, designated the transonic area rule, permits, within limits, an estimation of the drag-rise characteristics of wing-body combinations from the drag characteristics of a body of revolution having the same axial distribution of area (equivalent body). Area-distribution principles have also been used to correlate the drag increment occurring with installation of external stores and nacelles, references 2 and 3.

Examination of the axial area diagrams of the basic wing-body and the semielliptical shaped, sweptback wing-root inlet configurations of reference 4 showed that the inlet installation caused increases in cross-sectional area in a region where the area of the basic wing-body combination was a maximum. It was desired, therefore, to determine whether the principles of the transonic area rule could be applied to the inlet configuration to improve the transonic drag characteristics and in particular to eliminate the small increment in drag caused by the inlet installation for some portions of the transonic speed range. In the present investigation, the test configuration was obtained by indenting the fuselage of the wing-root inlet configuration to eliminate the increment in effective area added to the basic wing-body combination by the inlet installation. The tests were conducted in the Langley transonic blowdown tunnel through a Mach number range from 0.65 to 1.40 and angles of attack and mass-flow ratios from 0.5° to 6.7° , and 0.67 to 0.95, respectively. Lift, external-drag, and pitching-moment results are compared with those of the original inlet and basic wing-body configurations of reference 4.

SYMBOLS

C_{D_b}	drag coefficient of basic body of revolution
$C_{D_{wb}}$	drag coefficient of basic wing-body combination
$\Delta C_{D_{ext}}$	the difference in drag coefficient obtained between the inlet and basic configurations after the effects of the internal flow and air exit have been removed from the inlet configurations (see appendix of ref. 5)
C_{L_b}	lift coefficient of basic body of revolution
$C_{L_{wb}}$	lift coefficient of basic wing-body combination
$\Delta C_{L_{ext}}$	the difference in lift coefficient obtained between the inlet and basic configurations after the effects of the internal flow and air exit have been removed from the inlet configurations (see appendix of ref. 5)
$C_{M_{wb}}$	pitching-moment coefficient of basic wing-body combination taken about quarter-chord position of mean aerodynamic chord
ΔC_M	the difference in pitching-moment coefficient between the inlet and basic configurations after the effects of the air exit installation have been removed

$\frac{m_i}{m_o}$	mass-flow ratio, defined as the ratio of total internal mass flow to the mass flow through a free-stream tube equal in area to that of the minimum projected area at the inlet
A	area
c	local chord
\bar{c}	mean aerodynamic chord of the basic wing (4.462 in.)
M	Mach number
m	mass rate of internal flow
q	dynamic pressure
R	Reynolds number (based on \bar{c})
ρ	mass density
S	basic wing area (80.7 sq in.)
t	wing section thickness, percent c
α	angle of attack
Subscripts:	
i	inlet
o	free-stream
x	exit

APPLICATION OF TRANSONIC AREA RULE
TO AIR-INLET CONFIGURATIONS

In attempting to apply the principles of the transonic area rule to the present inlet configuration, the concept of equivalent area distribution was considered for inlets in general. As is stated in the introduction, the area rule permits, within limits, an estimation of the transonic drag rise of a wing-body combination from that of a body of revolution having the same axial distribution of cross-sectional area (equivalent body). In the case of an air-inlet configuration, however,

it is not obvious that the area rule can be applied to obtain bodies without internal air flow which will have drag-rise equivalence, or in what manner the area rule should be applied. The following brief discussion considers the problem of application of the area-rule concepts to several inlet configurations.

Consider first an ideal air-inlet configuration that has equal entrance and exit areas and has no momentum and pressure changes of the internal flow (inlet mass-flow ratio of 1.0), figure 1(a). For this case, it would appear logical that if a nonducted body were designed to have an axial area distribution equal to the total area distribution of the inlet configuration less the free-stream tube area, or, in this case, the equal entrance area, the streamlines at some distance from the nonducted body would be displaced in about the same manner as the corresponding streamlines for the inlet configuration and near transonic drag-rise equivalence should be attained.

Application of the area rule in this manner to inlet configurations of different geometry, however, might result in bodies which do not have drag-rise equivalence. Consider, for example, a wind-tunnel inlet model having internal losses but also having the exit area larger than the inlet area to permit operation at an inlet mass-flow ratio of unity. The nonducted body in this case would have a blunt base (fig. 1(b)). The external drag rise of the inlet model (external drag defined in the usual manner to be consistent with jet-engine thrust) and the blunt-based nonducted model (with base pressure converted to free-stream static pressure) should be very nearly equivalent except for possible effects of differences in base pressure on the external flow. Numerous experimental investigations, however, have shown that base-pressure variations generally affect the external flow only in limited regions near the body base and, therefore, usually have only minor effects on external drag.

Consider, further, the same inlet model operating at some reduced inlet mass-flow ratio. If, as in the cases above, the free-stream tube area is subtracted from the physical area of the inlet configuration, the nonducted body will have a blunt nose as well as a blunt base, figure 1(c). Further differences in drag-rise equivalence might be expected due to the blunt nose and a modified method of applying the area-rule concepts should perhaps be considered - one which assumes that the outermost external streamlines containing the internal flow are solid boundaries. In this case, removing the free-stream tube area from the axial area distribution of the inlet configuration including the external compression streamlines at mass-flow ratios less than unity would result in a nonducted body having the blunt nose replaced by a cusp-shaped nose (shown dotted in fig. 1(c)), which would vary both in length and shape with variations in mass-flow ratio and Mach number. It is not obvious which of these two methods will produce nonducted bodies having the closest drag-rise equivalence for the case of reduced mass-flow ratios. The only experimental information

available at present is contained in reference 6, where the transonic drag-rise characteristics of a blunt-nose and blunt-base nonducted body are compared with those of a nose-inlet configuration operating at a mass-flow ratio of about 0.7. These results indicate, qualitatively at least, close agreement between the inlet configuration and the blunt nose, nonducted body.

Consider, finally, an inlet configuration which has an exit area smaller than the inlet area and has the internal losses overcome by an internal pump in the case of a wind-tunnel model, or by a turbo-jet engine in the case of an actual airplane configuration. Application of the transonic area rule in the previously specified manner to this configuration when operating at a mass-flow ratio of unity will result in a nonducted body having negative area for some portions of the afterbody, figure 1(d). Such a configuration is obviously a physical impossibility. At some reduced mass-flow ratio, the equivalent nonducted body base area will become positive and drag-rise equivalence probably will be attained subject to the conditions previously discussed for the other configurations.

It appears from the preceding discussion that additional experimental information is needed in order to establish the details of the correct method for applying the transonic area rule to a ducted body, particularly in the regions near the inlet and outlet. For cases in which the mass-flow and the inlet-exit area ratios are both near unity, however, the drag-rise characteristics of the ducted body appear to correspond closely to those of a solid body having local cross-sectional areas equal to the corresponding local total cross-sectional areas of the ducted body less the area of the entering free-stream tube. In attempting to improve the transonic drag characteristics of the present sweptback wing-root inlet configuration, therefore, the fuselage was indented an amount equal to the total cross-sectional area added to the basic wing-body combination by the inlet installation less the area of the design entering free-stream tube.

MODELS

Details of the inlet and the basic wing-body configurations, investigated and reported in reference 4, are presented in tables I and II. Photographs of the two models are shown in figures 2(a) and 2(b). The basic model consisted of a wing with 45° quarter-chord sweep mounted with zero incidence in the midwing position on a fuselage of fineness ratio 6.7. The basic wing was composed of NACA 64A008 airfoil sections in the stream-wise direction and had an aspect ratio of 4.032, a taper ratio of 0.6, no twist, and no dihedral. The basic fuselage was formed by rotating an NACA 652A015 airfoil about its chord line.

~~CONFIDENTIAL~~

Provision for installation of the inlet in the wing root was accomplished by increasing the wing root quarter-chord sweep, the thickness ratio, and chord as shown in table I. The inlet lip sections were faired from the basic-wing leading-edge location to the maximum thickness of the modified wing root sections as shown in table II; inlet asymmetry and a lower lip stagger of 30° were incorporated to improve the external and internal flow performance, respectively, at high angles of attack.

Axial distributions of cross-sectional area for the inlet and basic configurations, figure 3(a), show that installation of the inlet caused a large bump in the distribution of the physical area, in a region where the area of the basic configuration was a maximum; it is noted from the previous section, however, that the physical or total area distribution for an air-inlet configuration does not, in itself, determine the external transonic drag-rise characteristics. The effective area distribution of the inlet configuration, as obtained by removal of the entering free-stream tube area from the total area diagram of the inlet configuration, is presented in figure 3(b); the area removed was equal to the entrance area times the design mass-flow ratio of 0.80, reference 4.

Equalizing the area diagrams of the inlet and basic models would require removing area from the inlet configuration between fuselage stations 5.00 and about 11.40 and adding area between stations 11.40 and 16.00, the exit station of the model. In modifying the present inlet model, however, the fuselage was indented to remove the excess area only, figure 4. The resulting area diagram was substantially the same as for the basic configuration for fuselage stations from 0 to 11.40. Small variations from an exact agreement were due to fairing the original fuselage shape to the indented portion of the fuselage between fuselage stations 5.00 and 6.00 and rearward of station 11.00. A photograph of the inlet configuration with indented fuselage is shown in figure 2(c).

APPARATUS AND TESTS

The tests were conducted in the Langley transonic blowdown tunnel at stagnation pressures ranging from 40 to 60 lb/sq in. abs. Lift, drag, pitching moment, and the pressure forces and internal momentum forces were measured in the same manner as those in reference 4. The force data for the inlet and indented configurations have been corrected for internal flow and the effect of the jet exit in accordance with the method presented in reference 5.

The range of test variables and the estimated maximum error in measured coefficients are given in the following tables:

Variable	Range	Maximum estimated error
M_0	0.65 to 1.41	± 0.01
R	5.5×10^6 to 7.4×10^6	At any M_0 , R varied approx. ± 2 percent due to changes in stagnation temperature
α	0.5° to 6.7°	$\pm 0.1^\circ$
m_1/m_0	0.67 to 0.95	± 0.02

Measured coefficient	Maximum estimated error of measured coefficient
ΔC_D	± 0.001
ΔC_L	± 0.01
ΔC_m	± 0.003

RESULTS AND DISCUSSION

Wind-tunnel wall interference.- Measured forces for the model investigated were influenced at supersonic speeds by wind-tunnel wall reflections of the model compression and expansion waves, as discussed in reference 5. Reflection of these waves to the test configuration caused abrupt changes in the drag-coefficient variations with Mach number unlike those obtained in free air. Inasmuch as the greatest changes occurred between Mach numbers of about 1.08 and 1.22, figure 5, in which range the reflected waves intersected the fuselage, it was thought that the fuselage alone was a major contributor to these abrupt changes. Subtraction of the drag coefficients measured on the fuselage alone from the drag coefficients of the wing-fuselage configurations of reference 4 and the present configuration resulted in drag-coefficient variations with Mach number, figure 6(a), that peaked initially at a Mach number of about 1.03, which is more nearly representative of the variations in free air.

Although subtraction of the measured fuselage-alone drag coefficients removes the largest part of the effect of the reflected waves, the resultant drag coefficients still contain the effects of the reflections on the

wings so that the absolute values of drag coefficient at Mach numbers greater than 1.08 are still not exactly equivalent to free-air values. The increments in drag coefficient between the various configurations, however, should be valid at Mach numbers greater than 1.22 inasmuch as configuration changes in the inboard sections would not be expected to cause any measurable change in the effects of the reflections on the outboard wing sections. At Mach numbers between 1.08 and 1.22, where the reflected waves intersect the inboard sections of the model, changes in configuration may cause some change in the effects of the reflections. It is believed, however, that the incremental changes in drag coefficient between configurations are at least of the correct order. The curves of figures 6 and 7 are dotted in the Mach number range from 1.08 to 1.22.

Effects of body indentation on aerodynamic characteristics.- The force coefficients of the indented inlet configuration have been plotted in figure 6 at two angles of attack for comparison with the basic and inlet configurations of reference 4. At the lowest angle, 0.1° , comparison of the three models shows that the drag break occurred at about the same Mach number (0.925) and the drag-rise characteristics were about the same for Mach numbers up to about 1.00. For Mach numbers above about 1.03 and to the maximum of the tests, the drag coefficients for the indented configuration were less than for the other two configurations. The maximum reductions occurred at a Mach number of 1.30, and the coefficients were about 0.005 and 0.006 less than for the inlet and basic configurations, respectively.

At an angle of attack of 4.2° , fuselage indentation reduced the increment in peak drag ($M \approx 1.02$) between the inlet and basic configurations only slightly. For Mach numbers above about 1.25, the indented inlet configuration had lower drag than either the inlet or basic configuration; the reduction, however, was somewhat less than that obtained at 0.1° . The lift coefficients for the indented configuration at $\alpha = 4.2^\circ$ were greater than for the inlet or basic configurations at Mach numbers above 0.95 (fig. 6(b)). It would be desirable, therefore, to compare the drag coefficients for the three configurations at the same values of the lift coefficient. The drag coefficients have been replotted in figure 7 at lift coefficients for the inlet configuration corresponding to angles of attack of 0.1° and 4.2° . It should be noted that the lift coefficient was not constant through the Mach number range, but that the drag coefficients for each configuration are for the same lift coefficient at any specified Mach number.

Comparisons at the lower lift coefficients, figure 7, show no significant change from the constant-angle-of-attack comparisons of figure 6(a). At the higher lift coefficients, however, fuselage indentation nearly eliminated the increment in peak drag between the inlet and basic configurations. At Mach numbers above 1.06 and to the maximum of the tests, the indented configuration had drag coefficients lower than those for

either the basic or inlet configuration with a maximum reduction of about 0.006 to 0.007 at $M \approx 1.25$. In addition to the reductions shown for the indented configuration, it appears from the shape of the drag-coefficient curves in the region of the highest test Mach number that body indentation would continue to be effective to speeds somewhat higher than the present test limit for both nonlifting and moderate-lifting conditions.

Pitching-moment coefficients for the indented configuration at the four test lift coefficients are compared with those for the basic and inlet configurations in figure 8. At the two extremes of the test Mach number range, indentation caused no changes in the pitching-moment characteristics obtained for the basic and inlet configuration. In the intermediate Mach number range, where installation of the inlet on the basic wing-body combination caused some interference in pitch, indentation tended to eliminate the interference.

SUMMARY OF RESULTS

An investigation has been conducted in the Langley transonic blow-down tunnel to determine whether the principles of the transonic area rule could be used to improve the transonic drag characteristics of a semielliptical shaped sweptback air inlet installed in the root of a 45° sweptback-wing-body combination. The results are briefly summarized below:

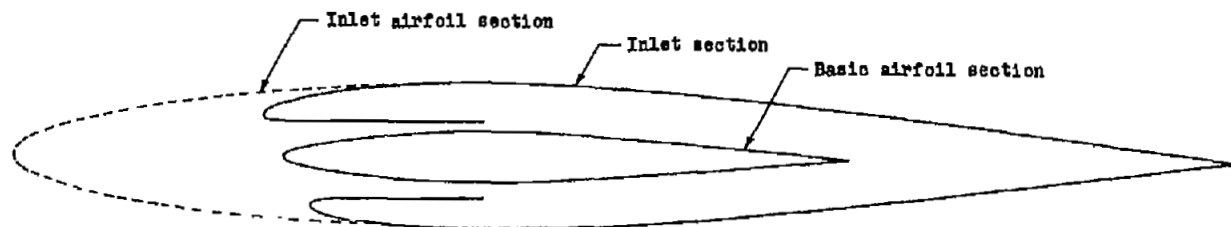
1. Indenting the fuselage of the inlet configuration eliminated the small increment in transonic drag coefficient caused by the inlet installation at both nonlifting and moderate-lifting conditions.
2. For Mach numbers above about 1.03 and to the maximum of the tests (1.4), the drag coefficients for the indented inlet configuration were lower than for either the basic or inlet configuration at the same lift coefficients.
3. The trends of the drag-coefficient curves in the vicinity of the maximum test Mach number indicate that body indentation may be effective in reducing the inlet configuration drag coefficient to Mach numbers somewhat greater than 1.4.

Langley Aeronautical Laboratory,
National Advisory Committee for Aeronautics,
Langley Field, Va., January 19, 1954.

REFERENCES

1. Whitcomb, Richard T.: A Study of the Zero-Lift Drag-Rise Characteristics of Wing-Body Combinations Near the Speed of Sound. NACA RM L52H08, 1952.
2. Smith, Norman F., Bielat, Ralph P., and Guy, Lawrence D.: Drag of External Stores and Nacelles at Transonic and Supersonic Speeds. NACA RM L53I23b, 1953.
3. Hoffman, Sherwood, and Wolff, Austin L.: Transonic Flight Tests To Determine Zero-Lift Drag and Pressure Recovery of Nacelles Located at the Wing Root on a 45° Sweptback Wing and Body Configuration. NACA RM L53H20, 1953.
4. Howell, Robert R., and Trescot, Charles D., Jr.: Investigation at Transonic Speeds of Aerodynamic Characteristics of a Semielliptical Air Inlet in the Root of a 45° Sweptback Wing. NACA RM L53J22a, 1953.
5. Howell, Robert R., and Keith, Arvid L., Jr.: An Investigation at Transonic Speeds of the Aerodynamic Characteristics of an Air Inlet Installed in the Root of a 45° Sweptback Wing. NACA RM L52H08a, 1952.
6. Walters, Richard E.: Application of Transonic Area Rule to a Sharp-Lipped Ducted Nacelle. NACA RM L53J09b, 1954.

TABLE I- DESIGN DIMENSIONS OF BASIC AND DUCTED WING

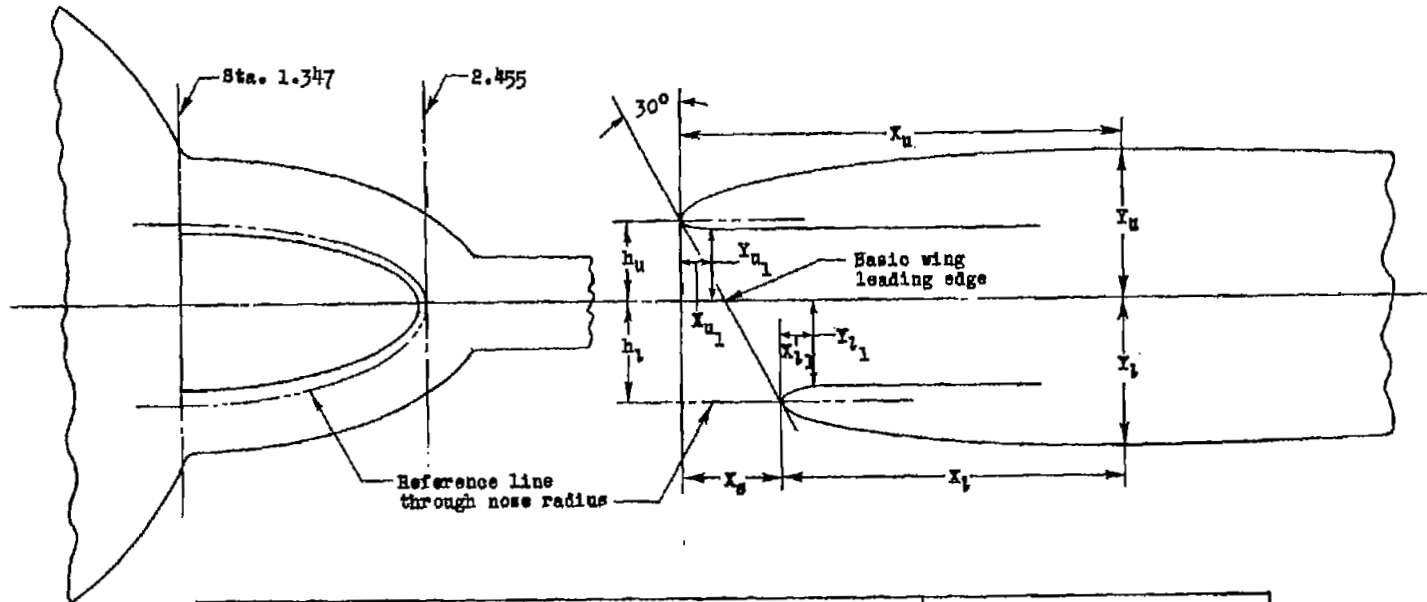


Semispan wing station (in.)	Basic wing			Ducted wing				
	c (in.)	t (percent c)	c/4 sweep	Total c (in.) (a)	t (percent total c)	c/4 sweep	Inlet c (in.)	t (percent inlet c)
0	5.587	8	45°					
1.347	5.250	8	45°	11.250	11.11	60°	8.777	14.24
1.500	5.212	8	45°	10.522	11.80	60°	8.334	14.90
1.750	5.150	8	45°	9.331	12.83	60°	7.608	15.75
2.000	5.087	8	45°	8.141	13.59	60°	6.883	16.07
2.250	5.025	8	45°	6.951	13.74	60°	6.157	15.53
^b 2.455	4.973	8	45°	5.976	12.78	60°	5.562	13.74
2.677	4.918	8	45°	4.918	8.00	60°	4.918	8.00
3.000	4.837	8	45°	4.837	8.00	45°	4.837	8.00
3.284	4.766	8	45°	4.766	8.00	45°	4.766	8.00
3.347	4.750	8	45°	4.750	8.00	45°	4.750	8.00
4.500	4.462	8	45°	4.462	8.00	45°	4.462	8.00
9.000	3.337	8	45°	3.337	8.00	45°	3.337	8.00

(a) Chord before installation of inlet
 (b) Outboard end of inlet

TABLE II- DESIGN DIMENSIONS OF WING ROOT INLET CONFIGURATION

(All dimensions in inches)

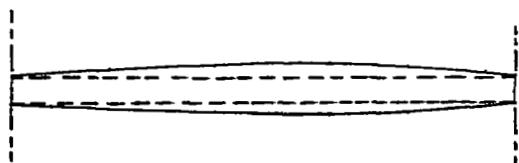


Wing station	External surfaces (a)							Internal surfaces (a)			
	h_u	X_u	Y_u	X_s	h_i	X_i	Y_i	X_{u_1}	Y_{u_1}	X_{i_1}	Y_{i_1}
1.347	0.338	1.998	0.625	0.442	0.428	1.556	0.626	0.125	0.300	0.185	0.366
1.500	.334	2.003	.621	.437	.423	1.567	.621	.125	.296	.185	.361
1.750	.314	2.004	.599	.411	.398	1.593	.599	.125	.278	.185	.338
2.000	.273	1.991	.553	.357	.345	1.635	.553	.125	.238	.185	.289
2.250	.195	1.960	.478	.256	.248	1.705	.478	.125	.161	.185	.196

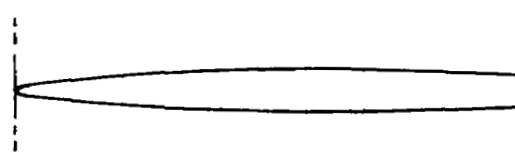
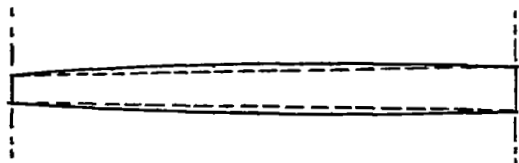
(a) External and internal nose shapes determined from elliptical ordinates

Nose inlet configuration

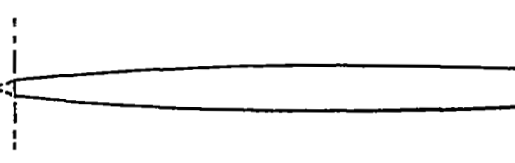
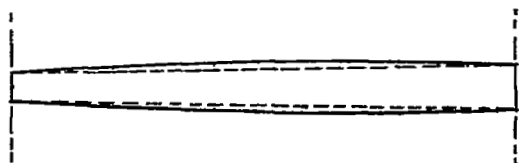
Nonducted body



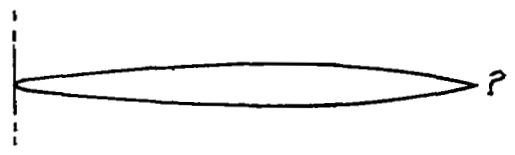
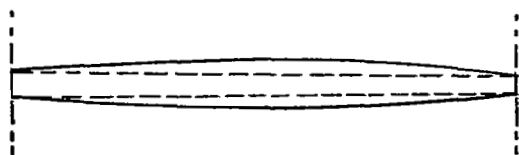
(a) Ideal configuration; $\frac{A_x}{A_i} = 1.0$; $\frac{m_i}{m_o} = 1.0$.



(b) Practical configuration; $\frac{A_x}{A_i} > 1.0$; $\frac{m_i}{m_o} = 1.0$.

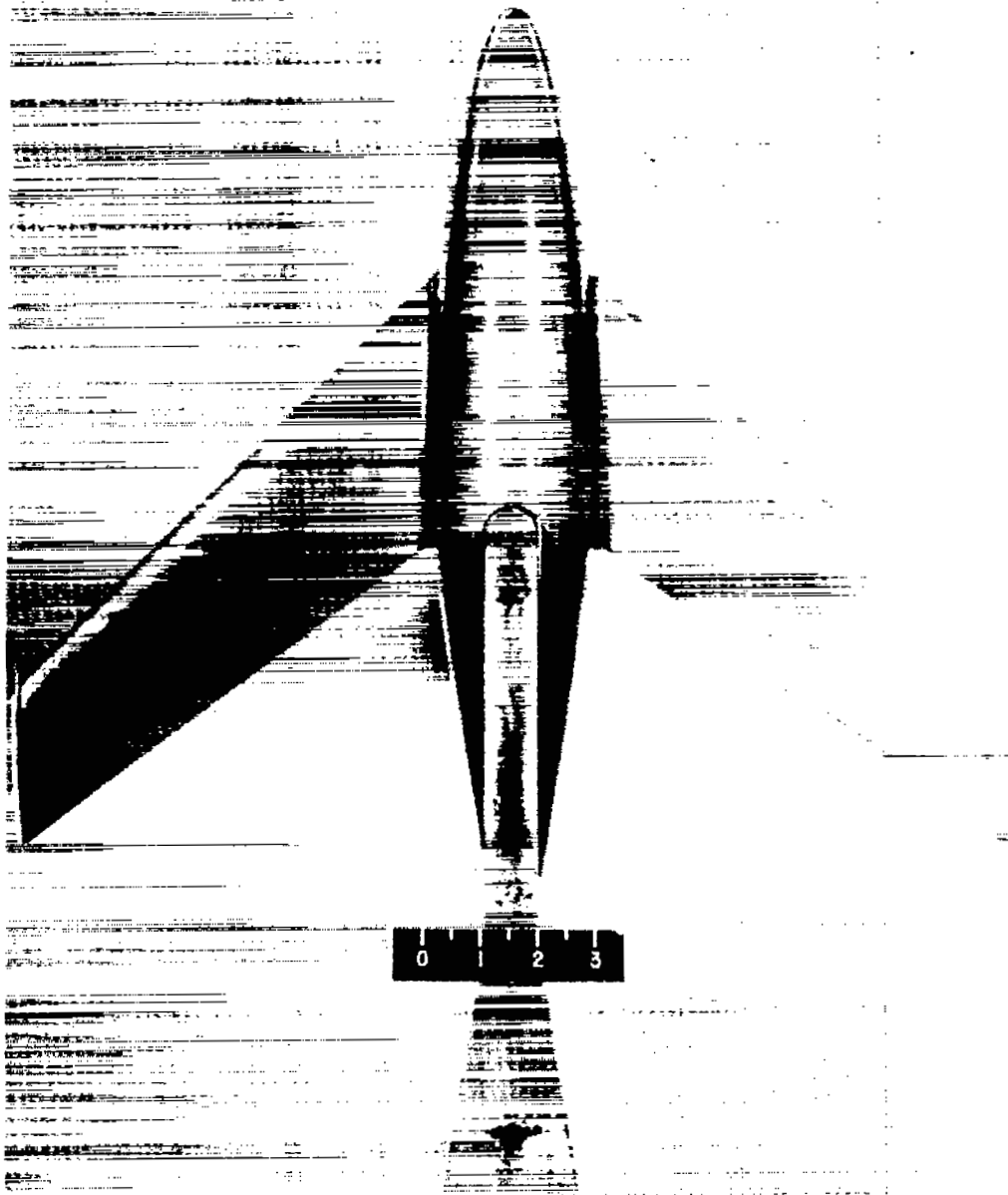


(c) Practical configuration; $\frac{A_x}{A_i} > 1.0$; $\frac{m_i}{m_o} < 1.0$.



(d) Practical configuration; $\frac{A_x}{A_i} < 1.0$; $\frac{m_i}{m_o} = 1.0$.

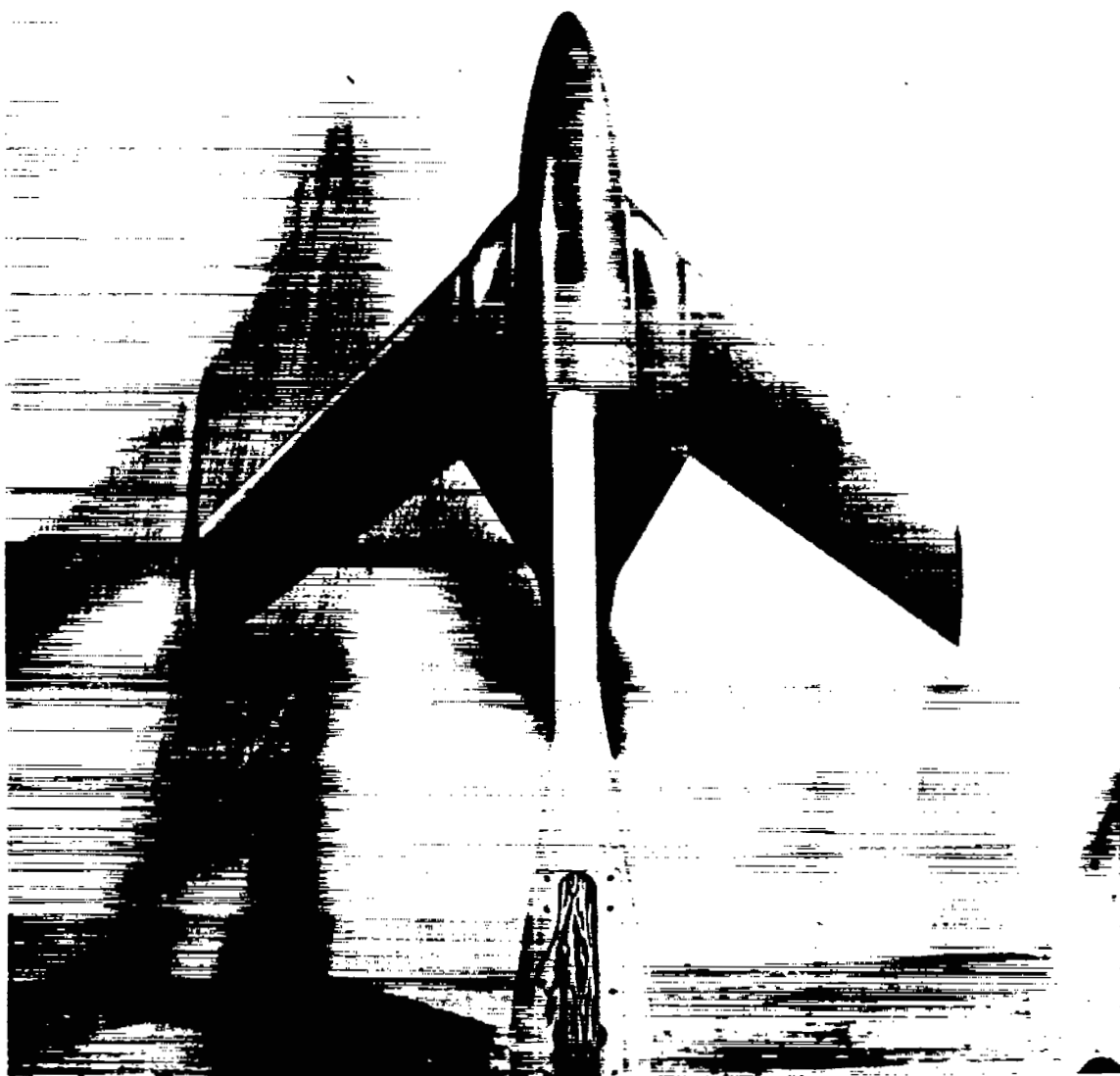
Figure 1.- Sketches illustrating application of transonic-area-rule concepts to air-inlet configurations.



(a) Basic wing-body configuration.

L-78978

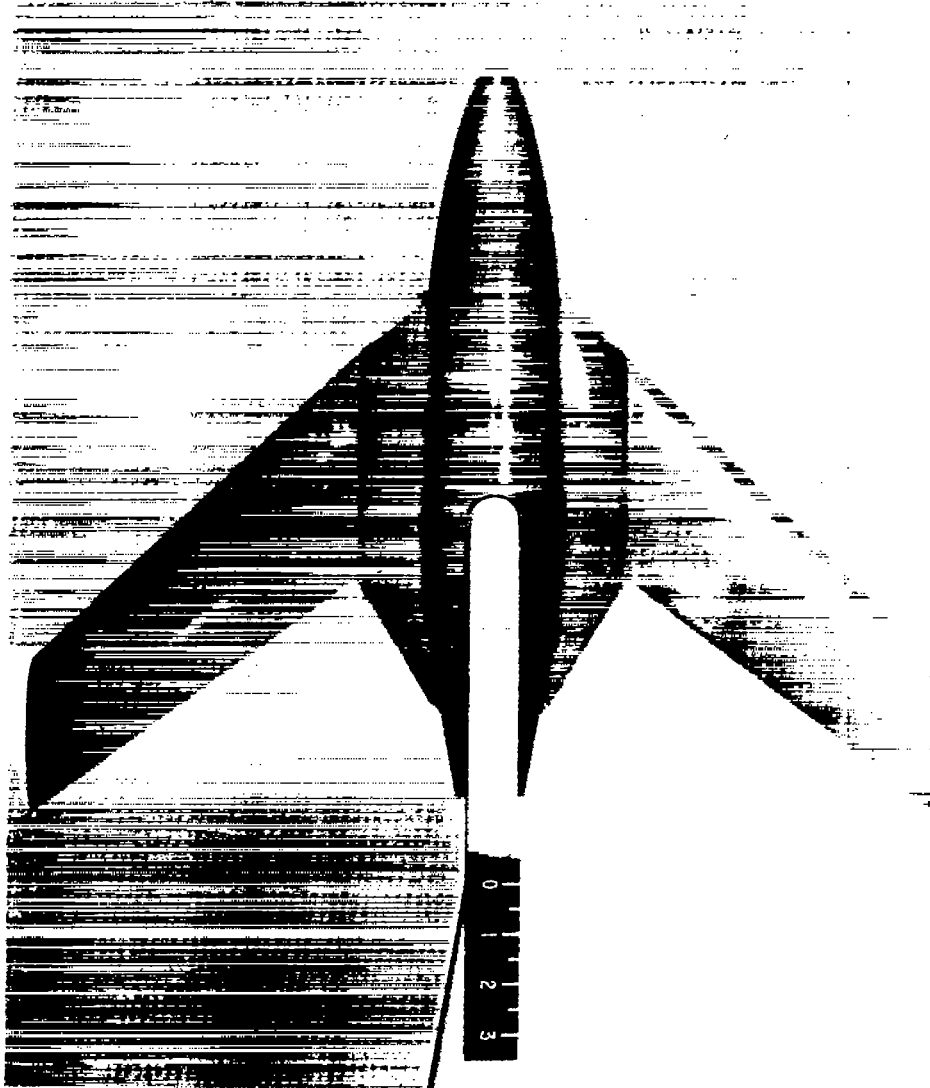
Figure 2.- Photographs of the three test configurations.



(b) Inlet configuration.

L-76796

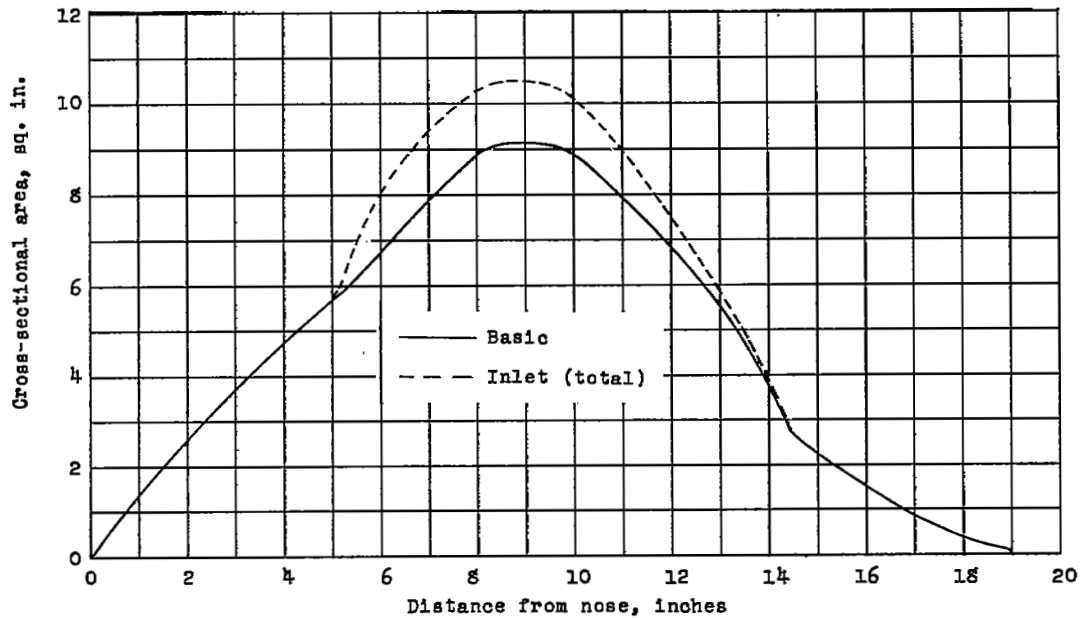
Figure 2.- Continued.



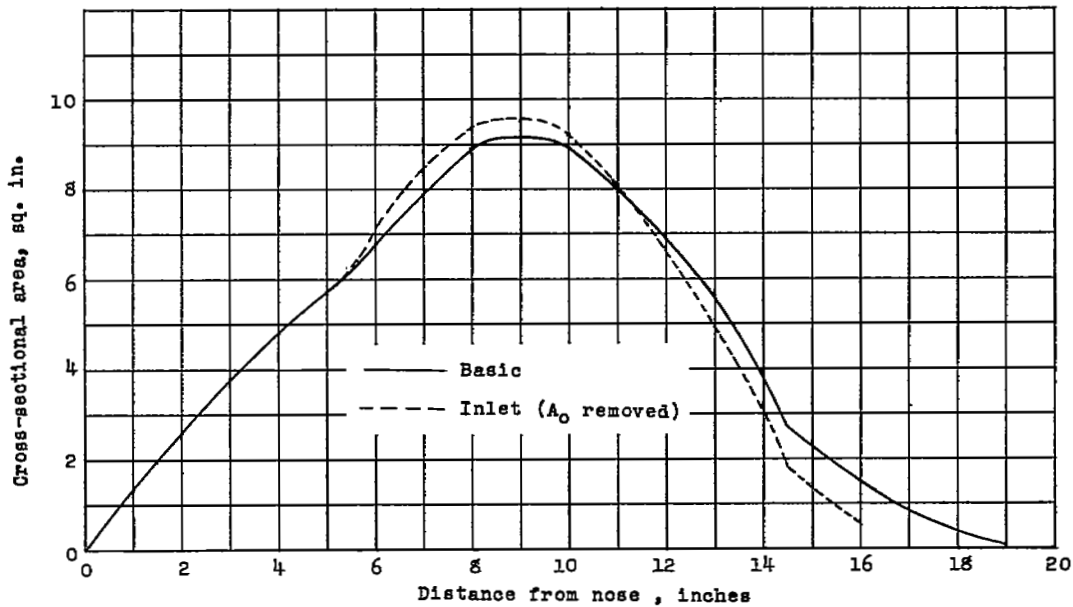
(c) Indented inlet configuration.

L-80688

Figure 2.- Concluded.



(a) Basic configuration and inlet configuration (total).



(b) Basic configuration and inlet configuration with A_0 removed.

Figure 3.- Axial distribution of cross-sectional area of the basic and inlet configurations.

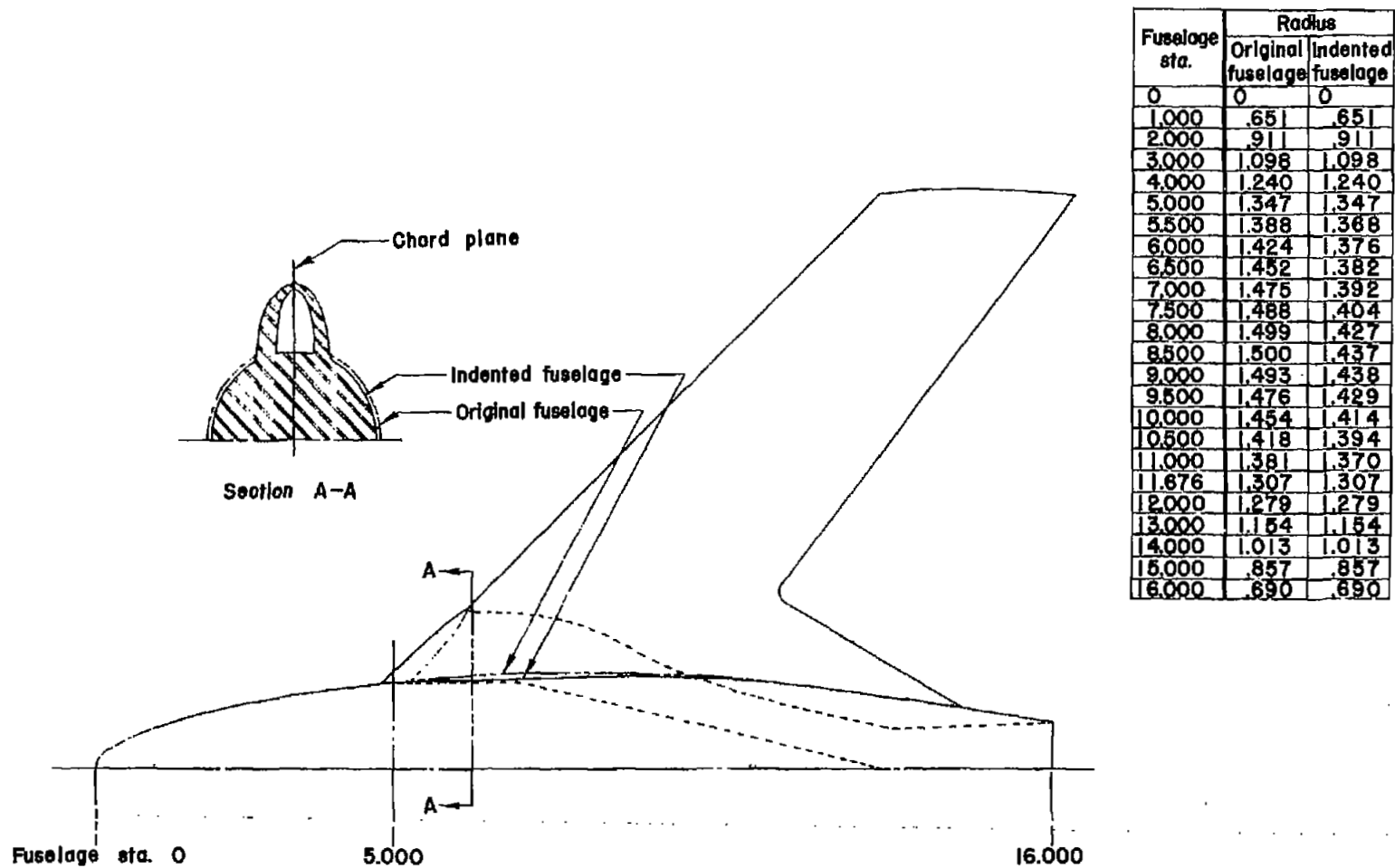
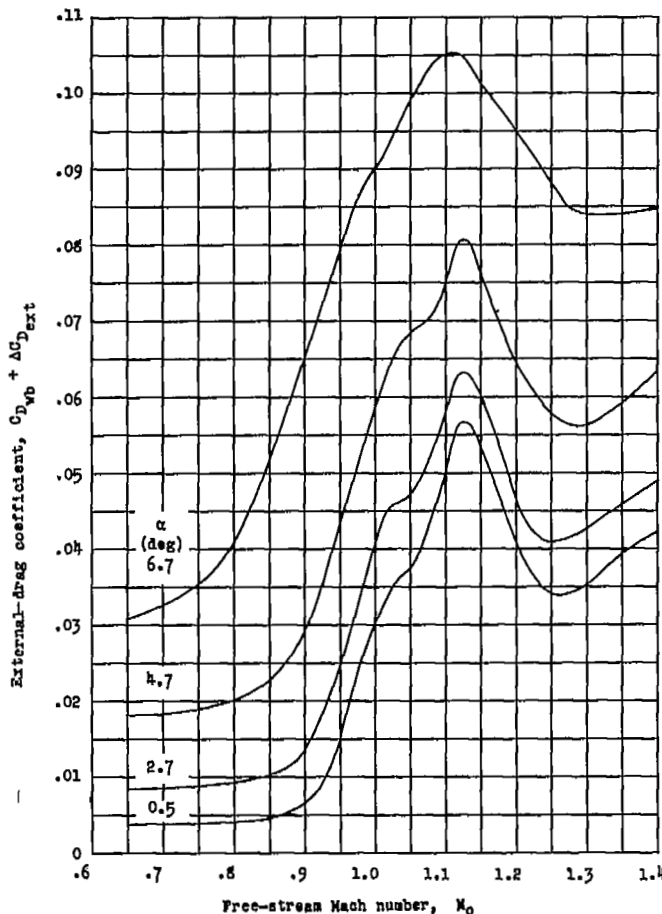
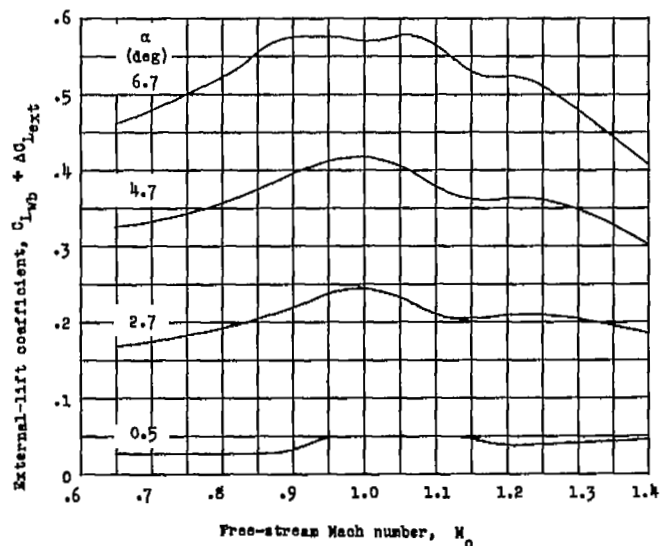


Figure 4.- Plan view of indented inlet configuration with dimensions of original and indented fuselage.

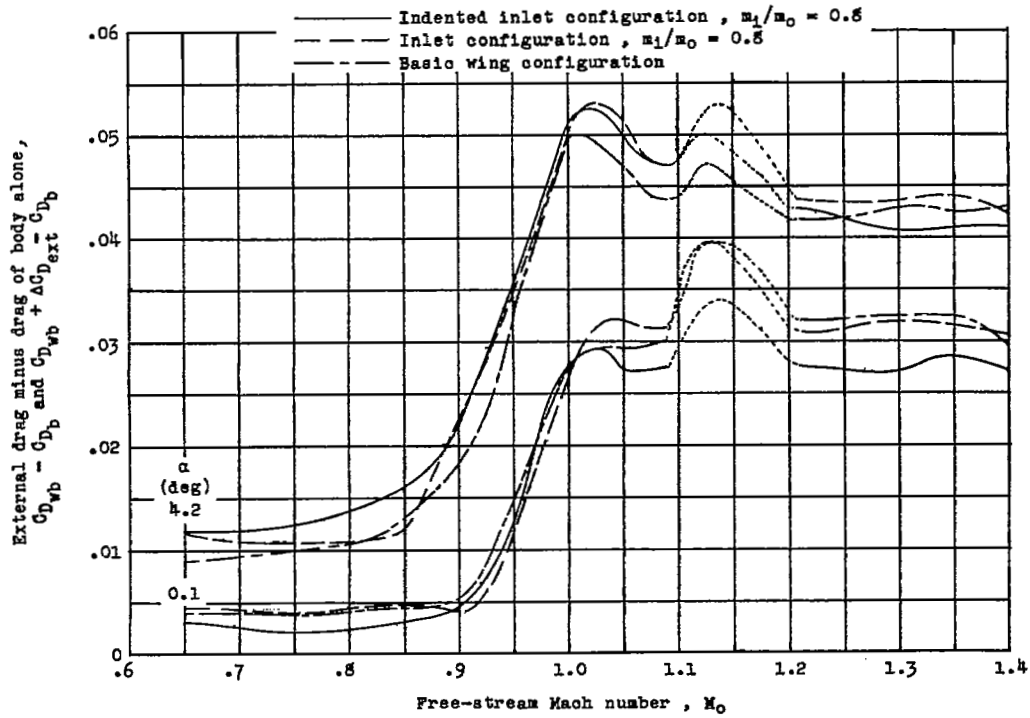


(a) External-drag coefficient.

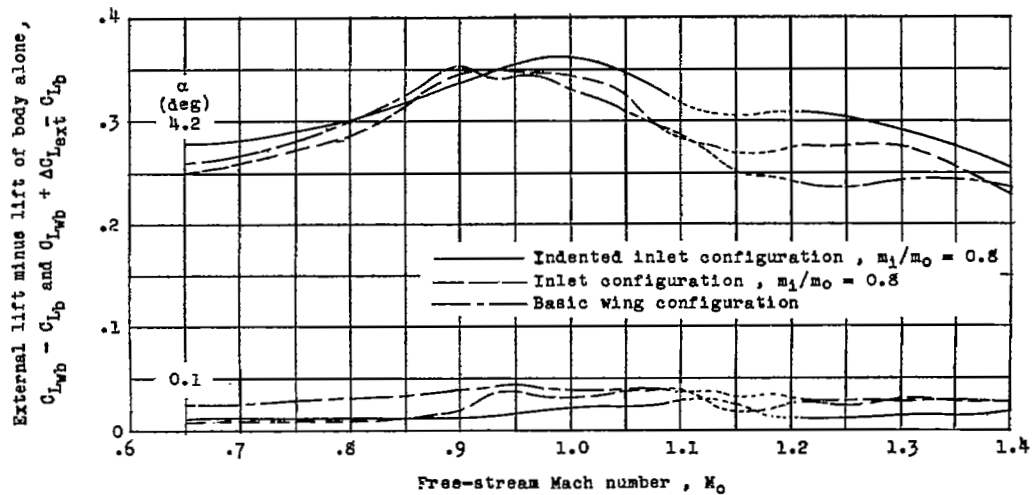


(b) External-lift coefficient.

Figure 5.- External-drag and external-lift coefficients of the indented inlet configuration as a function of free-stream Mach number.
 $\frac{m_1}{m_0} = 0.80.$



(a) External-drag coefficients.



(b) External-lift coefficients.

Figure 6.- Comparison of increments in external-drag and external-lift coefficients of the three configurations over the test Mach number range at 0.1° and 4.2° angles of attack.

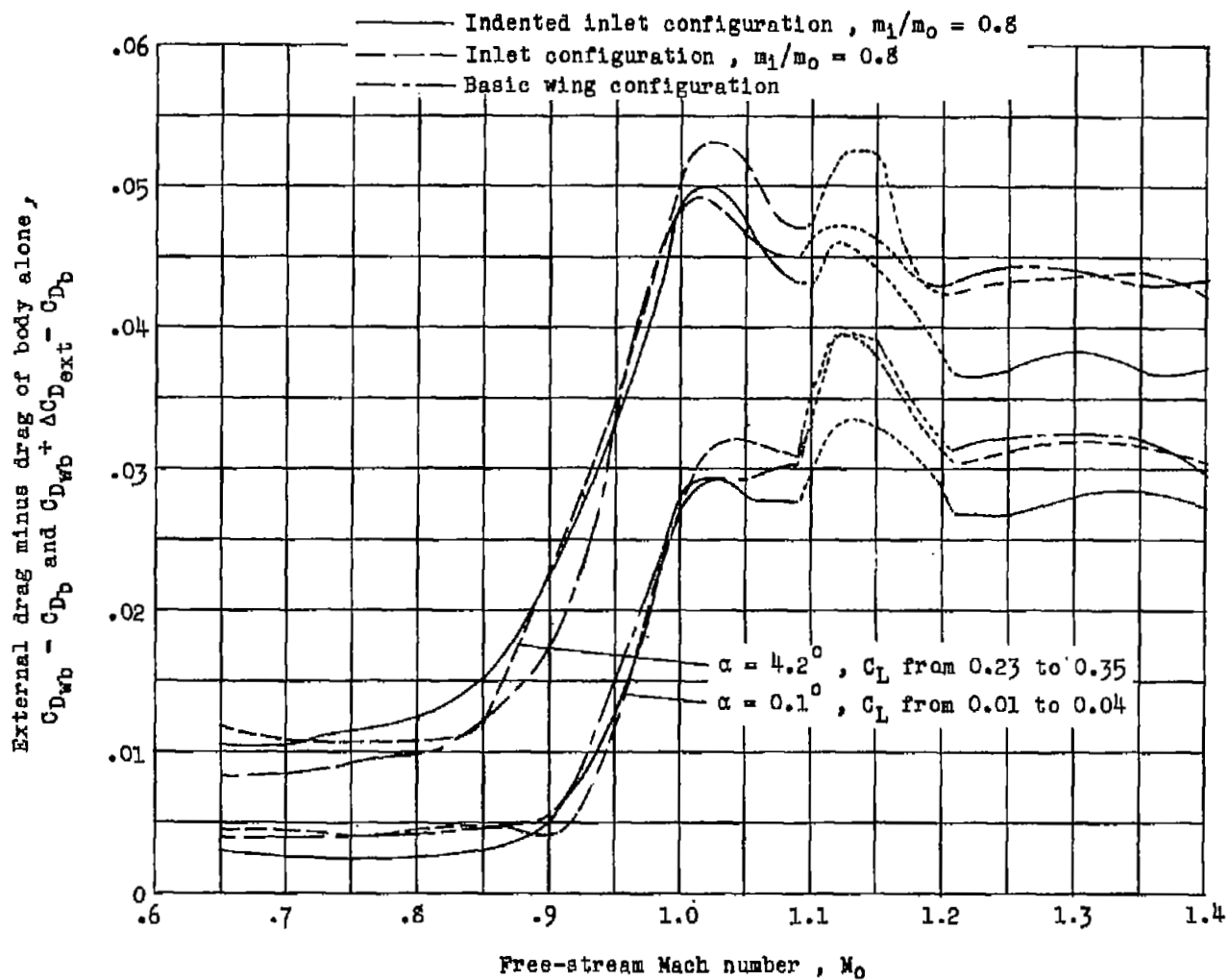


Figure 7.- Comparison of external-drag-coefficient increments of the three configurations at lift coefficient increments obtained for the inlet configuration at 0.1° and 4.2° angles of attack.

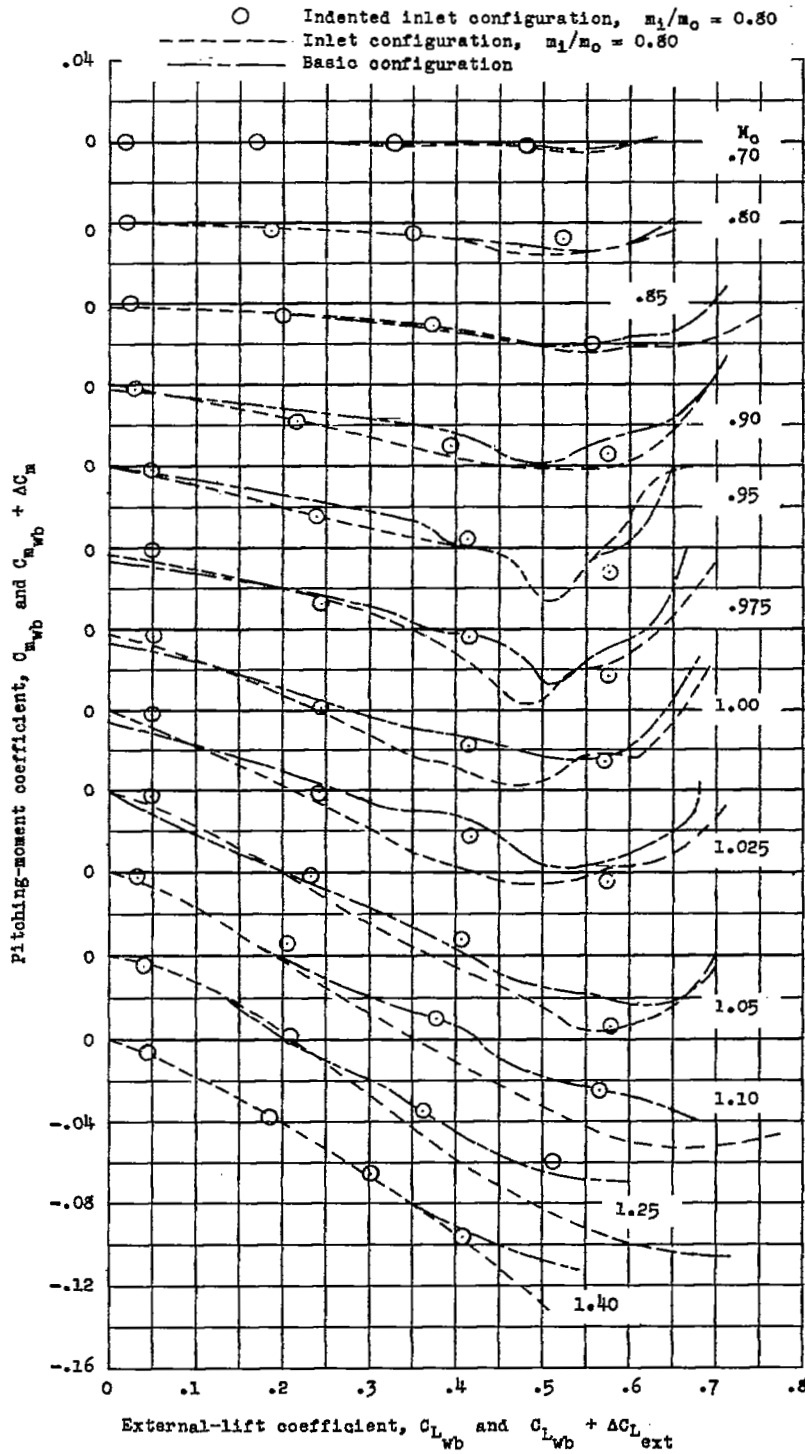


Figure 8.- Comparison of pitching-moment coefficients of the three test configurations for the test range of lift coefficients and Mach numbers.